2014 IEEE International Conference on Robotics & Automation (ICRA)
Hong Kong Convention and Exhibition Center
May 31 - June 7, 2014. Hong Kong, China

Active Tethered Pelvic Assist Device (A-TPAD) to Study Force Adaptation in Human Walking

Vineet Vashista, *Student Member, IEEE,* Xin Jin, *Student Member, IEEE,* and Sunil K. Agrawal, *Member, IEEE*
Robotics and Rehabilitation (ROAR) Laboratory, Mechanical Engg., Columbia University, New York, NY 10027
{vv2233, xj2146 and sunil.agrawal}@columbia.edu

***Abstract*—An active Tethered Pelvic Assist Device (A-TPAD) has been presented in this paper. TPAD is a cable robot for studying force adaptation in human walking by applying external forces and moments on the human pelvis. A two stage control strategy was implemented to apply the desired force-moment profile. The controller includes (i) a quadratic programming based optimization scheme, (ii) a real-time human motion monitoring system and (iii) a PID feedback loop to plan and implement the required cable tensions. The control strategy was validated first by testing it on a dummy pelvis setup. A pilot experiment was then conducted with a human walking on a treadmill with A-TPAD. The goal was to apply a vertical downward force vector equivalent to 10% of subject's body weight (BW) at the pelvis. Results showed that the applied vertical force was acting downwards over the full gait cycle and was between 8-13% of the BW. Other force-moment components were maintained within a specified range during the experiment. Increased foot pressure was reported in the presence of vertical force. In summary, A-TPAD provides the capability of applying and controlling a desired force-moment profile on the human pelvis over a gait cycle.**

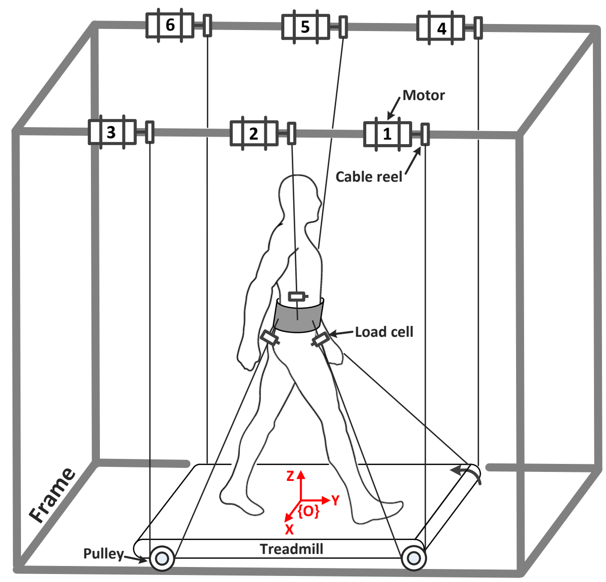

Fig. 1. Schematic of the active Tethered Pelvic Assist Device (A-TPAD). Motors were mounted on a rigid frame and cables were routed using pulleys to the subject's pelvis. Global coordinate system, $\{O\} : XYZ$, was set at the center of the treadmill.

I. Introduction

Post stroke survivors, children with cerebral palsy, persons with lower extremity amputation and persons living with traumatic brain injury are among the population groups who have been identified to have asymmetry in gait pattern as well as reduced weight-bearing capabilities [1]–[5]. Such impaired walking not only affects the quality of life but also adds to the risk of falling and serious injuries. Therefore, strategies to improve such walking conditions are quite important in rehabilitation.

In recent years, many experimental paradigms have been developed to study motor adaptation and to improve human gait. Such paradigms apply external perturbations to human walking, which result in kinematic errors while walking. Human nervous system minimizes these errors through recalibration of motor commands. Such recalibrations of established motor behaviors represent motor adaptation and hold great potential in gait rehabilitation [6], [7].

Several robotic devices have been used to study motor adaptation and encouraging results were reported in the literature [8]–[15]. However, some of these devices affect human dynamics in an undesirable manner because of their intrinsic dynamics due to large moving inertia. In [16], it was reported that a robot could affect subjects' gait significantly if it adds more than 6 kg mass on the human pelvis. Similar inertia effects on stability of leg kinematics were reported in [17].

Cable robots intrinsically have low weight and add minimal dynamics to that of the human. However, since a cable can only pull but not push, these cable robots have been mostly used in body weight suspension paradigm. In such cases, human weight helps to keep the cables taut. The Zero-G [18] and NaviGAITor [19] are some of the multi-directional support systems for over-ground walking.

Our group has recently developed a passive Tethered Pelvic Assist Device (TPAD), to study force adaptation in human walking [20]–[22]. It can apply different force-moment profiles on a subject's pelvis. In [20], vertical downward force was applied on the human pelvis such that healthy subjects showed adaptation in their gait kinematics and kinetics. Such paradigms can have positive impact on human weight bearing capabilities. In [21], asymmetric forces were applied in the transverse plane on the human pelvis. Healthy subjects adapted to these forces by exhibiting asymmetric gait patterns. Such paradigms can help improve gait symmetry. These studies show that TPAD can be used to design subject-specific experiments and has the potential to improve impaired walking patterns.

In this work, we propose an active TPAD (A-TPAD) to apply controlled force-moment on human pelvis. In experiments with the passive TPAD, it was observed that the force-moment profile changed with the subject's motion. For example in [20], the external vertical force acted downwards only during the single support phase of the gait cycle. The advantage of A-TPAD is that it can maintain a prescribed force-moment profile over the complete gait cycle. A two stage control strategy in force mode has been implemented. CAREX, an upper arm rehabilitation device developed by our group [23], is the only other cable robot available in literature to use force mode control strategy. One challenge for the A-TPAD is to keep the cables attached to the pelvis taut during the gait cycle. As seen in Fig. 1, both upward and downward pelvic motion can lead to cable slackening. Therefore, a human motion monitoring system was included in the high level controller to continuously plan the desired cable tension values. In this work, an experiment was first conducted on a dummy pelvis to validate the control strategy. An experiment with a single subject walking on a treadmill at constant speed has also been reported in this paper.

II. System Design and Model

A. Experimental Setup

The passive Tethered Pelvic Assist Device (TPAD) has been described in authors' previous works [20]–[22]. Active TPAD (A-TPAD) builds upon the same structure with the objective to control the applied force-moment profile on the human pelvis. The motors, controller and other hardware components are shown in Figs. 1 and 2. Each cable connects to a hip brace worn by the subject. The other end of the cable connects to a motor mounted on an inertially fixed frame. A tension sensor was installed in series with each cable to measure the instantaneous tension. Each tension sensor can record up to 890 N and is powered using a 12 V DC amplifier (MLP-200 and TMO-1 from Transducer Techniques, California). AC servo motors with encoders were powered in torque mode (Goldline XT motors and Servostar CD drivers from Kollmorgen, Pennsylvania). Pulleys were used to appropriately route the cables from the motors to the pelvis. The design allows using any number of motors and to change the locations of motors and pulleys to achieve different cable configurations. All motors were direct drive with rated continuous torque of 2.7 Nm. A cable reel of 72.39 mm diameter on each motor shaft was used so that a maximum continuous tension of 75 N could be achieved. These reels prevent the cables from wrapping upon itself, as described in [24]. A motion capture system (Bonita-10 series from Vicon, Denver) was used to track the cable attachment points on the hip brace during the experiment. The control was implemented using Labview, PXI real time controller and data acquisition cards (National Instrument, Austin).

Dummy Pelvis Experiment: The controller was first tested on a dummy pelvis, which consisted of two 1 ft by 1 ft square Delrin® plates attached together with a six axis force-torque sensor (Mini45 from ATI Industrial Automation, North Carolina), as shown in Fig. 2. The force-torque sensor was

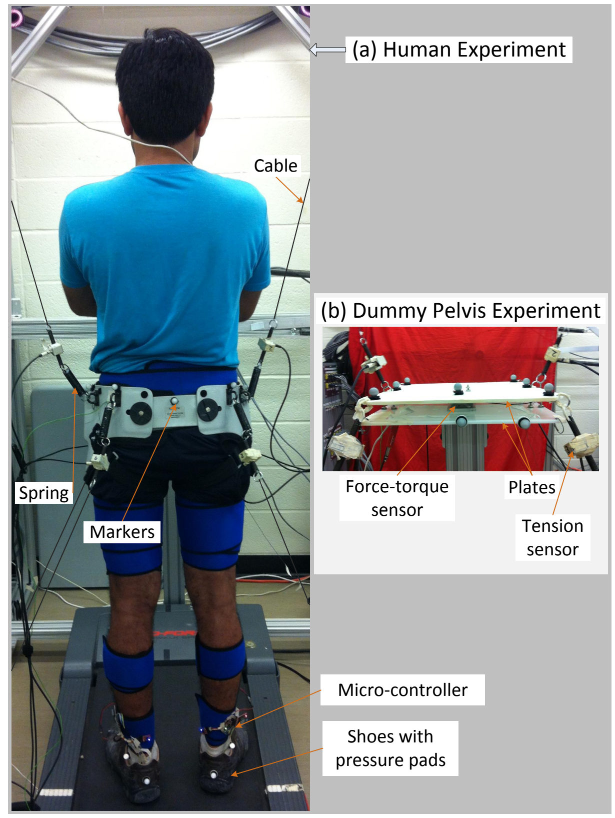

Fig. 2. Experimental setup includes six motors mounted on a rigid frame, a ten cameras motion capture system, tension sensors to record cable tensions and a real time controller. (a) Human Experiment - Cables were attached to a hip brace, when the subject walked on a treadmill at a constant speed. Shoes with pressure pads were used to record the foot pressure data. (b) Dummy Pelvis Experiment - Two plates setup was used to represent human pelvis. Cables were attached to the upper plate, while the lower plate was set in motion. A six axis force-torque sensor, rigidly connected to both plates, recorded the force-moment vector at the center of the upper plate with respect to the lower plate.

rigidly attached to the two plates and recorded the force-moment vector at the center of the upper plate with respect to the lower plate. The cables from the motors, in series with tension sensors, were attached to the upper plate. During the experiment, a person held the lower plate using attached handle bars to set it in motion. Reflective markers were placed on the upper plate to record the cable attachment points. Three reflective markers were also placed on the lower plate to record the motion of the lower plate in the global coordinate system. This information was used to resolve the force-moment vector measured using the force-torque sensor in the global coordinate system.

Human Experiment: The controller was also tested with a human walking on a treadmill at a constant speed of 3.2 $kmph$. A spring with 2.28 N/mm stiffness value was added between the hip brace and the tension sensor in each cable. Shoes with pressure pads and micro-controller were also used to record the foot pressure values during walking (Fig. 2). Similar micro-controllers were used to record foot pressure data in passive TPAD experiments [20], [21].

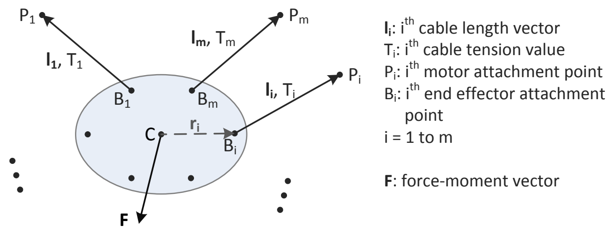

Fig. 3. A n degrees of freedom cable robot with m cables. One end of each cable is attached to the end effector and the other end to a motor, shown as B_i and P_i respectively.

For both experiments, six motors were used to control the tension in the six cables. The cable configuration was similar to the loading configuration as described in [20]. Four cables were routed from the bottom of the frame while the other two were attached to the top of the frame, as shown in Fig. 1. Pulleys were provided on the frame to route the cables from the motors. The goal of the experiments was to apply a constant vertical downward force F_z at the center of the upper plate and at the pelvic center. The other force-moment vector components were kept within a specified limit.

B. Tension Planner

For a rigid body with n degrees of freedom, $n = 3$ for planar and $n = 6$ for spatial. If m actuated cables are used, these cables will apply an external $n \times 1$ force-moment vector **F**, as shown in Fig. 3. This vector can be expressed in terms of $m \times 1$ cable tension vector T and the system geometry.

$$AT = F, \tag{1}$$

where A is a $n \times m$ structure matrix which depends on the system geometry and can be computed knowing the coordinates of the cables' attachment points. For a six degrees of freedom system ($n = 6$), when **F** is computed at point C. The matrix A can be expressed as

$$A = \begin{bmatrix} \dots & \hat{\mathbf{l}}_i & \dots \\ \dots & \mathbf{r}_i \times \hat{\mathbf{l}}_i & \dots \end{bmatrix}_{6\times m}, \tag{2}$$

where $\hat{\mathbf{l}}_i$ is the i^{th} unit cable length vector oriented away from the connecting rigid body and $\mathbf{r}_i$ is the vector from the point C to the i^{th} cable attachment point on the rigid body.

In the case of A-TPAD, the goal is to apply a particular $n \times 1$ force-moment vector on the human pelvis. As shown earlier, at least $n+1$ cables would be required for generating the desired $n \times 1$ **F** vector [25], [26]. This makes Eq. (1) under-determined. The general solution can be written in terms of the minimum norm solution ($\overline{T}$) and the null space of structure matrix A, assuming A to be full rank [27].

$$T = \overline{T} + N(A)\lambda, \tag{3}$$

where

$$\overline{T} = A^T(AA^T)^{-1}F, \tag{4}$$

$N(A)$ is the null space of matrix A and λ is an arbitrary $(m-n)$ vector.

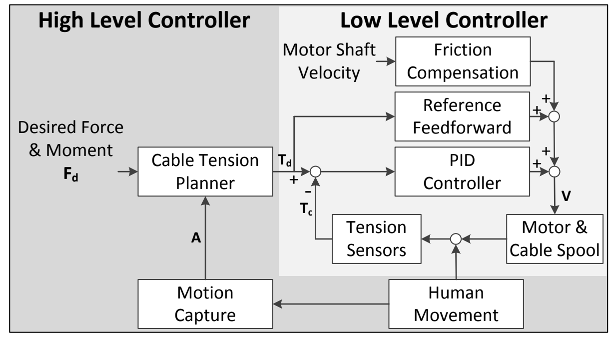

Fig. 4. Control of the A-TPAD was implemented using a high and a low level control structure. The high level controller plans the desired cable tension vector T_d to apply a desired force-moment vector F_d. The low level controller implements these cable tensions using a feedback PID loop and a reference feed-forward. A friction compensation model based on the motor velocity was also included in the low level controller.

For $T \geq 0$, Eq. (3) forms a convex region. Therefore, an optimization problem can be formulated to find the best solution within the feasible set. In the current work, a quadratic programming based optimization scheme with a lower and a upper bound on the cable tension values was implemented.

$$min f \tag{5}$$

$$f = \frac{1}{2}(T - T_p)^T(T - T_p)$$

$$s.t. \quad A_{eq}T = F_{eq}; \quad -F_{ieq} \leq A_{ieq}T \leq F_{ieq}$$

$$and \quad T_{min} \leq T \leq T_{max}$$

T_p is a positive constant, which is added to the objective function to ensure non-zero cable tension values. Here A_{ieq} denotes the i^{th} row of A and F_{ieq} the i^{th} element of F. During the experiments, F_{eq} was chosen such that a desired downward force is applied while other components were kept within a specified limit.

C. Controller

The control for A-TPAD can be broadly divided into two levels as shown in Fig. 4.

High Level Controller: This part of the controller plans the amount of tension to be generated in each cable to achieve the desired force-moment vector during the experiment. The locations of cable attachment points recorded using the motion capture system, were then used to form the structure matrix A, as described in Eq. (2). The motion capture system provided data at $250Hz$. The markers data was sent to Labview. A quadratic programming problem was formulated to calculate the desired cable tension T_d based on the desired force-moment vector F_d, as described in Eq. (5). The values of T_p were taken to be the cable tension values calculated in the previous step, to keep the cable tensions smooth. For those instances, when the optimization problem did not yield the solution, previously calculated tension values were used.

Low Level Controller: This part of the controller implemented the desired cable tension vector T_d calculated in the previous section. It involved a PID feedback loop based on the current cable tension values. PID gains were selected such that each motor step response had an overshoot below 15% and a rise time of 0.08 sec. A reference feedforward based on motor constants, which mapped the desired cable tension to the motor voltage, was also included. Voltage in small increments were applied to the motors and the corresponding cable tension values were recorded. A least square fit was then used to calculate the motor constant for each motor. It is important to note that for both PID gains and motor constant calculations the other end of each cable was connected to a inertially fixed point. A friction compensation based on motor speed was included in the low level controller. To estimate the friction compensation parameters, a linear model was developed between friction and motor speed, as described in [24]. Low level controller was implemented at $1000Hz$.

III. Results and Observations

The location of motors on the frame was decided by simulating Eq. (5) in Matlab (Math Works, Natick). A set of pelvic motion data with hip brace cable attachment points was captured using a motion capture system. For each frame, matrix A was calculated and Eq. (5) was solved to check the existence of feasible cable tension values. The location of each cable attachment point on the frame (P_i) is given in Table I. Global coordinate system $\{O\} : XYZ$ is shown in Fig. 1.

A. Dummy Pelvis Experiment

The purpose of this experiment was to validate the controller. For this experiment, the subject was asked to hold the lower plate and to move it in a circular path in the sagittal $Y-Z$ plane. The quadratic optimization in Eq. (5) was solved for the following parameters,

$$\left.\begin{array}{c} |F_x| \leq 5N \\ |F_y| \leq 10N \\ F_z = -35N \\ |M_{x,y,z}| \leq 2Nm \\ 5 \leq T \leq 40N \end{array}\right] \Rightarrow \begin{array}{c} F_{ieq} = \left[\begin{array}{ccccc} 5 & 10 & 2 & 2 & 2 \end{array}\right]^T \\ F_{eq} = -35 \\ 5 \leq T \leq 40 \end{array}$$

The force-moment vector at the center of the upper plate relative to the lower plate was recorded using a six axis force-torque sensor. These values were converted to global coordinate system using the lower plate marker data and are denoted as vector F_s. The force-moment vector at the center of the upper plate was also calculated using the cable tension values and the structure matrix A, Eq. (1), and is denoted

	$\mathbf{P}_1$	$\mathbf{P}_2$	$\mathbf{P}_3$	$\mathbf{P}_4$	$\mathbf{P}_5$	$\mathbf{P}_6$
X (m)	0.63	0.45	0.63	-0.63	-0.45	-0.63
Y (m)	1.07	0	-1.07	1.07	0	-1.07
Z (m)	0.11	2.43	0.11	0.11	2.43	0.11

TABLE I

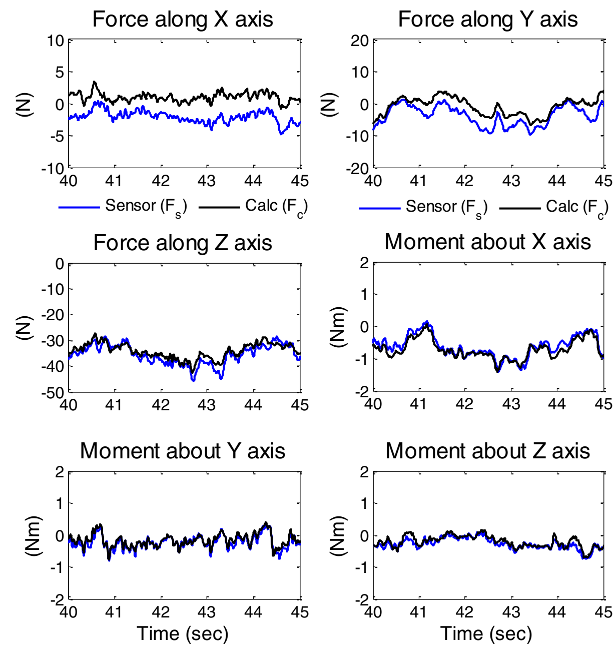

Fig. 5. The force-moment vector acting at the center of the upper plate measured using a force-torque sensor (F_s) and calculated using Eq. (1) (F_c) in global coordinate system over five seconds of the trial.

as F_c. The F_s and F_c values are shown in Fig. 5 for a part of the experiment. A close match among F_s and F_c force-moment values was observed, except for a small offset in the X direction force values. As seen in Fig. 2, ball type reflective markers were placed on the plate surface, as it was not possible to place these directly on the actual cable attachment location. This would generate a small error in the cable length vector estimation.

The results of this experiment were also used to verify whether the applied force-moment vector on the plate remained within the desired range during the plate motion. As seen in Fig. 5, the moment values were within the limit of $\pm 2Nm$ in the three directions. The force values in the X and Y directions were also within the desired limit of $\pm 5N$ and $\pm 10N$ respectively. The vertical force component along Z axis was expected to remained constant at -35 N. Small variations were observed in its values, similar variations can also be observed in other force-moment components. These variations in the force-moment values were the result of external human dynamics, which acted on the lower plate during the motion.

B. Human Experiment

During the human experiment, the subject was first asked to walk on a treadmill at an involving speed of 3.2 $kmph$ for one minute without any external forces. The subject wore the hip brace without any cables. This session was referred to as the baseline session. The cables were then attached to the hip brace. The external force profile was applied when the subject was standing still and straight on the treadmill. The subject was then asked to walk on the treadmill at the same speed for one minute with the applied force profile. This session was

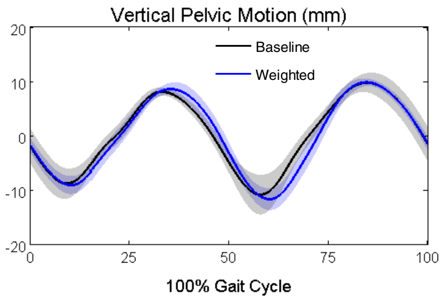

Fig. 6. Vertical pelvic motion averaged over the last ten gait cycles for baseline and weighted sessions. The shaded area shows the variability within the gait cycles. Each gait cycle was referenced based on right foot heel strike.

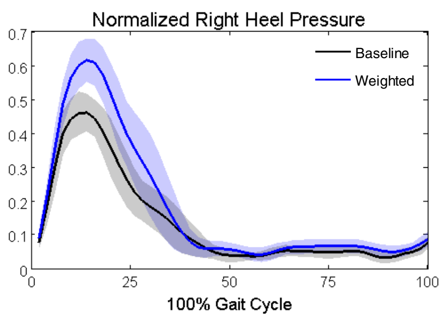

Fig. 7. Right heel pressure averaged over the last ten gait cycles for baseline and weighted sessions. The shaded area shows the variability within the gait cycles. A '0' value would mean no weight on the pressure pad while a '1' corresponds to the full scale reading.

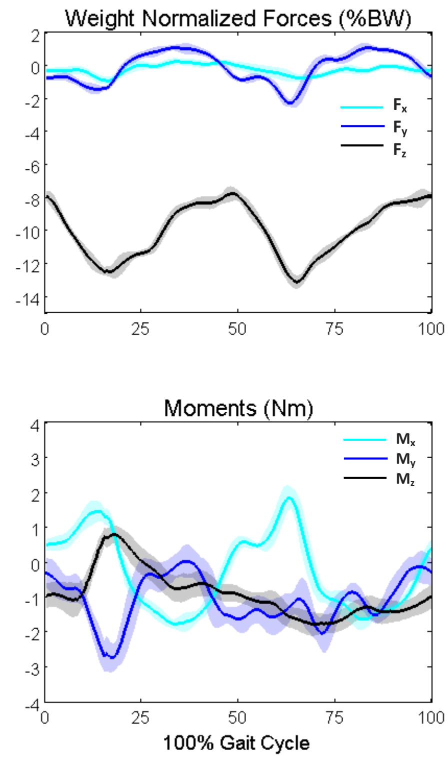

Fig. 8. The force-moment vector at pelvic center in the global coordinate system, calculated using Eq. (1) during the weighted session, averaged over the last ten gait cycles. Each gait cycle was referenced based on right foot heel strike.

referred to as the weighted session. The goal was to apply a vertically downward force equivalent to 10% of subject's BW at the pelvic center. The quadratic optimization in Eq. (5) was solved for the following parameters,

$$\left.\begin{array}{c} |F_x| \leq 5N \\ |F_y| \leq 10N \\ F_z = -70N \\ |M_{x,y,z}| \leq 2Nm \\ 5 \leq T \leq 40N \end{array}\right] \Rightarrow \begin{array}{c} F_{ieq} = \left[\begin{array}{ccccc} 5 & 10 & 2 & 2 & 2 \end{array}\right]^T \\ F_{eq} = -70 \\ 5 \leq T \leq 40 \\ Subject\ Weight = 70Kg \end{array}$$

The pelvis and the foot marker data were used to calculate the gait events. These event data were then used to divide the other sensor data in gait cycles, where each gait cycle was referenced based on right foot heel strike. Time histories of each data set were normalized in time to 100% gait cycle. In the following section, averaged data from the last ten gait cycles of the baseline and the weighted sessions have been presented.

The motion of the pelvic center in the vertical direction over a gait cycle is presented in the Fig. 6. The pelvic center was calculated as the mid-point of two pelvic markers in the human frontal plane. It was observed that the pelvic vertical motion between the baseline and the weighted sessions was within the variability of ten gait cycles; and no differences were observed between the two sessions. The results presented in the passive TPAD experiment with loading configuration reported reduction in the vertical upward motion of the pelvis during the single support phases of the gait cycle [20]. In the A-TPAD, the other end of each cable is attached to a motor and not to a fixed point, which was the case in passive TPAD setup. Since, motors were controlled in force mode, the subject was able to execute the full range of pelvic vertical motion over the complete gait cycle. Ability to allow unconstrained limb motion is a desirable feature for any rehabilitation robot.

The right heel pressure data is shown in Fig. 7. It was observed that the pressure values increased during the weighted session when compared to the baseline session values. This result is in accordance with the results presented in the passive TPAD study with vertical downward force on pelvis [20]. Such a change was expected since there was an extra downward force on the subject pelvis during the weighted session. The pressure pads used in this experiment had a limit of 45.4 kg. Since, these pads only covered a fraction of the human foot quantitative analysis was not conducted.

Figure 8 plots the force-moment vector at the pelvic center during a gait cycle calculated as per Eq. (1). Cables were not attached to the hip brace during the baseline session, therefore only the weighted session data are presented. The force values were normalized with the human weight. The moment values were within the desired limit, except M_y which developed a small offset in the negative direction. The vertical force values varied from $8\%BW$ to $13\%BW$ with roughly twice the gait frequency, though the variability within the gait cycles was significantly small. The force values along X and Y directions were within $\pm 2\% BW$. The variations in the force-moment values during a gait cycle could be attributed to the unaccounted human dynamics during walking. Passive TPAD experiment with loading configuration in [20] reported that the external vertical force acted downwards only during the single support phases of the gait cycle. In the current experiment, the external vertical force acted downwards over the complete gait cycle. Therefore, the active version of TPAD provides the capability of controlling and maintaining the applied external forces, though small variations in magnitude were observed due to unaccounted human dynamics.

IV. Conclusion and Future Work

An Active TPAD (A-TPAD) was designed and successfully tested for applying controlled force-moment profile on the human pelvis. A validation experiment was first conducted on a dummy pelvis. A reasonably close match was observed between the measured and the calculated force-moment vector at the plate center. These results validated the two-stage control strategy adapted for A-TPAD. A human experiment was also conducted. The goal was to apply a vertical downward force vector equivalent to 10% of subject's BW on the pelvis when the subject walked on a treadmill. The applied vertical force component was between 8-13$\%$ of the BW and the vertical pelvic range of motion was not affected significantly. The other force-moment components were maintained within a small range. This work represents successful implementation of A-TPAD.

In future, studies will be conducted with healthy and impaired population groups using A-TPAD to extend the usefulness of TPAD in the realm of motor adaptation.

V. Acknowledgment

Partial support of NIH grant number HD38582 and NSF IIS-1339666 are gratefully acknowledged.

References

[1] Olney, S.J., Costigan, P.A. and Hedden, D.M., *Mechanical Energy Patterns in Gait of Cerebral Palsied Children with Hemiplegia*, Physical Therapy, vol. 67, pp. 1348–1354, 1987.

[2] Zamparo, P., Francescato, M.P., De Luca, G., Lovati, L. and di Prampero, P.E., *The energy cost of level walking in patients with hemiplegia*, Scand J Med Sci Sports, 5, pp. 348–352, 1995.

[3] Mattes, S.J., Martin, P.E., and Royer, T.D., *Walking symmetry and energy cost in persons with unilateral transtibial amputations: Matching prosthetic and intact limb inertial properties*, Archives of Physical Medicine and Rehabilitation, vol. 81, pp. 561–568, May 2000.

[4] Olney, S.J. and Richards, C., *Hemiparetic gait following stroke. Part I: Characteristics*, Gait & Posture, 4, pp. 136–148, 1996.

[5] Balasubramanian, C.K., Bowden, M.G., Neptune, R.R. and Kautz, S.A., *Relationship between step length asymmetry and walking performance in subjects with chronic hemiparesis*, Arch. Phys. Med. Rehabil., vol. 88, pp. 43-49, 2007.

[6] Martin, T.A., Keating, J.G., Goodkin, H.P., Bastian, A.J. and Thach, W.T., *Throwing while looking through prisms. II. Specificity and storage of multiple gaze- throw calibrations*, Brain, vol. 119, pp. 1199-1211, 1996.

[7] Bastian, A.J., *Understanding sensorimotor adaptation and learning for rehabilitation*, Current opinion in neurology, vol. 21, 2008.

[8] Lam, T., Anderschitz, M. and Dietz, V., *Contribution of Feedback and Feedforward Strategies to Locomotor Adaptations*, J Neurophysiol, vol. 95, pp. 766–773, 2006.

[9] Houldin, A., Luttin, K. and Lam, T., *Locomotor adaptations and after effects to resistance during walking in individuals with spinal cord injury*, J Neurophysiol vol. 106, pp. 247-258, 2011.

[10] Banala, S.K., Kim, S.H., Agrawal, S.K. and Scholz, J.P., *Robot Assisted Gait Training With Active Leg Exoskeleton (ALEX)*, IEEE Trans Neural Syst Rehab Eng, vol. 17, No. 1, 2009.

[11] Kim, S.H., Banala, S.K., Brackbill, E.A., Agrawal, S.K., Krishnamoorthy, V. and Scholz, J.P., *Robot-assisted modifications of gait in healthy individuals*, Exp Brain Res, vol. 202, pp. 809–824, 2010.

[12] van Asseldonk, E.H.F., Koopman, B., Buurke, J.H., Simons, C.D. and van der Kooij, H., *Selective and adaptive robotic support of foot clearance for training stroke survivors with stiff knee gait*, 11^{th} International Conference on Rehabilitation Robotics, Japan, June 23-26, 2009.

[13] Noble, J.W. and Prentice, S.D., *Adaptation to unilateral change in lower limb mechanical properties during human walking*, Exp Brain Res, vol. 169, pp. 482–495, 2006.

[14] Savin, D.N., Tseng, S.C. and Morton, S.M., *Bilateral adaptation during locomotion following a unilaterally applied resistance to swing in nondisabled adults*, Journal of neurophysiology, vol. 104(6), pp. 360011, 2010.

[15] Savin, D.N., Tseng, S.C., Whitall, J. and Morton, S.M., *Poststroke Hemiparesis Impairs the Rate but not Magnitude of Adaptation of Spatial and Temporal Locomotor Features*, Neurorehabilitation and Neural Repair, Feb 24, 2012.

[16] Meuleman, J., Terpstra, W., van Asseldonk, E., and van der Kooij, H., *Effect of added inertia on the pelvis on gait*, in Rehabilitation Robotics (ICORR), 2011 IEEE International Conference on., 2011, pp. 1–6.

[17] Arellano, C., O'Connor, D., Layne, C., and Kurz, M., *The independent effect of added mass on the stability of the sagittal plane leg kinematics during steady-state human walking*, Journal of Experimental Biology, vol. 212, no. 12, pp. 1965–1970, 2009.

[18] Hidler, J., Brennan, D., Black, I., Nichols, D., Brady, K., and Nef, T., *ZeroG: overground gait and balance training system*, J Rehabil Res Dev, vol. 48, no. 4, pp. 287298, 2011.

[19] Shetty, D., Fast, A., and Campana, C., *Ambulatory suspension and rehabilitation apparatus*, U.S. Patent 7 462 138, 2008.

[20] Vashista, V., Agrawal, N., Shaharudin, S., Reisman, D.S. and Agrawal, S.K., *Force adaptation in human walking with symmetrically applied downward forces on the pelvis*, IEEE Transactions on Neural Systems and Rehabilitation Engineering, Issue: 99, 2013 (in press).

[21] Vashista, V., Reisman, D.S. and Agrawal, S.K., *Asymmetric Adaptation in Human Walking using the Tethered Pelvic Assist Device (TPAD)*, in Proceedings of the IEEE International Conference on Rehabilitation Robotics (ICORR), 2013.

[22] Vashista, V., Mustafa, S.K. and Agrawal, S.K., *Experimental Studies On The Human Gait Using A Tethered Pelvic Assist Device (T-PAD)*, IEEE International Conference on Rehabilitation Robotics (ICORR), ETH Zurich Science City, Switzerland, pp. 1–6, 2011.

[23] Mao, Y., and Agrawal, S.K., *Transition from mechanical arm to human arm with CAREX: A cable driven ARm EXoskeleton (CAREX) for neural rehabilitation*, IEEE International Conference on Robotics and Automation (ICRA), pp. 2457-2462, 2012.

[24] Mao, Y., and Agrawal, S.K., *A Cable Driven Upper Arm Exoskeleton for Upper Extremity Rehabilitation*, IEEE International Conference on Robotics and Automation (ICRA), Shanghai, China, pp. 4163–4168, 2011.

[25] Ming, A. and Higuchi, T., *Study on multiple degree-of-freedom positioning mechanism using wires. I: Concept, design and control*, International journal of the Japan Society for Precision Engineering, 28(2):131–138, 1994.

[26] Mustafa, S. K. and Agrawal S. K., *On the Force-Closure Analysis of n-DOF Cable-Driven Open Chains Based on Reciprocal Screw Theory*, IEEE Transactions on Robotics, Vol. 28, No. 1, 2012, 22-31.

[27] Oh, S. and Agrawal, S., *Cable Suspended Planar Robots with Redundant Cables: Controllers with Positive Tension*, IEEE Transactions of Robotics, Vol. 21, No. 3, 2005, 457-465.